An Electromyographic Signal Acquisition System for Sarcopenia

Yihui Jian[1], Kaitai Mao[2], Jing Chen[3,4], Xinrui Ling[3], Ziguan Jin[1], Zhiqiu Ye[1], Geng Yang[1,5], Qin Zhang[3,4(✉)], and Kaichen Xu[1(✉)]

[1] State Key Laboratory of Fluid Power and Mechatronic Systems, School of Mechanical Engineering, Zhejiang University, Hangzhou 310000, China
xukc@zju.edu.cn
[2] School of Ocean Science and Engineering, Harbin Institute of Technology, Weihai, China
[3] Department of Geriatrics, First Affiliated Hospital, School of Medicine, Zhejiang University, Hangzhou, China
zhangqin1978@zju.edu.cn
[4] Key Laboratory of Diagnosis and Treatment of Aging and Physic-Chemical Injury Diseases of Zhejiang Province, School of Medicine, The First Affiliated Hospital, Zhejiang University, Hangzhou, Zhejiang, China
[5] Zhejiang Key Laboratory of Intelligent Operation and Maintenance Robot, Hangzhou, China

Abstract. Sarcopenia, characterized by age-related loss of strength and muscle mass, profoundly affects the elderly's well-being. Currently, diagnosing sarcopenia requires the utilization of extensive and cumbersome testing equipment. Surface electromyography (sEMG) is able to track muscle status and has been effectively employed in diagnosing various diseases or human-machine interactions, but its application in sarcopenia detection remains unexplored. In this study, a compact sEMG system is developed to monitor sarcopenia, which is endowed with compact dimensions, ease of operation, and wireless data transmission capabilities. The investigation involves the analysis of sEMG signals from 15 elderly participants. A significant correlation is established between the median frequency of these sEMG signals and the appendicular skeletal muscle mass (ASM). The proposed sEMG-based sarcopenia detection device exhibits the merit in portable use and highly operational efficiency. In future, it holds a high potential to replace the commercially cumbersome or non-portable testing devices, thereby facilitating widespread sarcopenia screening across diverse populations.

Keywords: Sarcopenia · sEMG · Wearable devices

1 Introduction

Sarcopenia is a newly defined disease in recent decades and has been paid great attentions. It is distinctly characterized by the age-related decline in skeletal muscle mass [1, 2], resulting in sluggish mobility and reduced strength among the elderly. Notably, it leads to muscle convulsions, spasms, falls, fractures, and other related complications [3, 4]. The influence of sarcopenia on human's health is profound, greatly compromising the living

quality of middle-aged and elderly people. More seriously, it can threaten their lives [5]. Fortunately, there are currently good nutritional interventions and exercise methods for sarcopenia to alleviate its deterioration. Therefore, a timely diagnosis of sarcopenia is necessary.

Currently, the diagnosis of sarcopenia needs a comprehensive evaluation including three key factors: muscle strength, physical performance, and ASM [6]. Muscle strength and physical performance can be measured simply by grip strength and gait speed, respectively. However, ASM requires the help of large instruments. The current optimal option to measure muscle mass relies on utilizing Dual-energy X-ray absorptiometry (DEXA), which is capable of precisely quantifying ASM. Limited by the high cost, bulky, and radiation, it is mainly used in the larger medical facilities. A suitable alternative to quantify the ASM is bioelectrical impedance analysis (BIA) [7], which offers greater user-friendliness. Nonetheless, fluctuations in cellular impedance that are highly related to body conditions greatly influence the test's accuracy, especially when the body suffers from dehydration or edema. Although lower cost is available for the BIA equipment, it is still not affordable for some community hospitals or individuals. Hence, it is of vital significance to design a simple, convenient, and economical ASM assessment tool for extensive sarcopenia screening [8, 9].
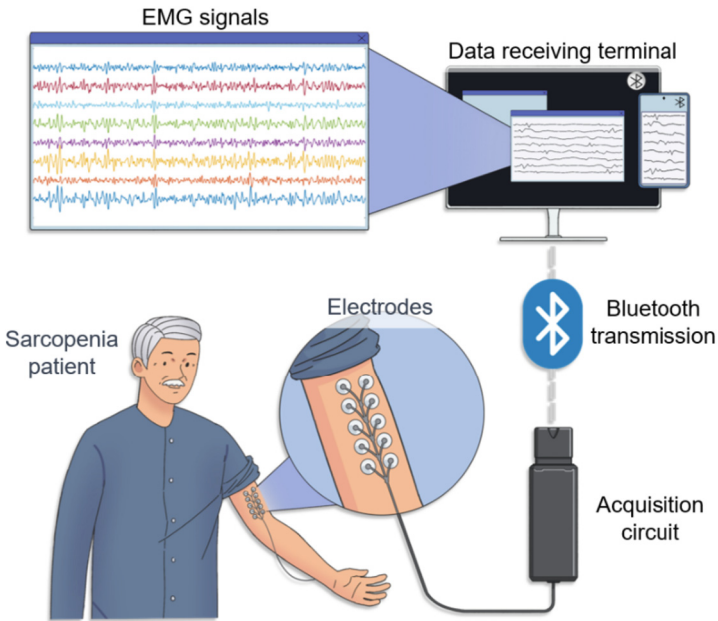
Fig. 1 An sEMG signal acquisition system for sarcopenia. It is composed of acquisition electrodes, an sEMG signal processing system, a mobile user interface with Bluetooth for wireless data transmission, and an sEMG-based sarcopenia analysis system

One promising approach is the use of sEMG to diagnose sarcopenia. It serves as a modality and technique capable of providing an objective representation of the bioelectrical activity within the neuromuscular system [10]. It shows the unique advantages of easy operation, non-invasive and multi-faceted target detection [11, 12]. The sEMG signals contain a wealth of information that reflect the muscle activities for effective diagnosis of sarcopenia. Until now, although a few investigations on sEMG signals have been conducted to diagnose various diseases like Parkinson's disease, cerebral palsy in children, and spinal cord injuries [13], a pragmatic and effective diagnostic approach for sarcopenia is still under exploration.

Here, an sEMG signal acquisition system tailored for sarcopenia detection has been proposed (Fig. 1). This system allows for the efficient acquisition of eight-channel sEMG signals and enables a comparable performance to commercial sEMG electrodes. Notably, it is equipped with a low-power Bluetooth module for wireless data transmission. Owing to its user-friendly operation and reliable performance, we established collaborations with a local hospital (The First Affiliated Hospital, Zhejiang University School of Medicine). This collaboration includes a data acquisition task of sEMG signals from 15 elderly participants. Subsequently, relevant feature signals have been extracted from these sEMG signals to reveal certain eigenvalues corresponding to muscle mass measurements obtained via BIA. Our proposed sEMG detection system offers a low cost, lightweight, multi-channel and highly efficient solution for sarcopenia identification in the future.

2   Acquisition System

2.1   Acquisition Circuit

To enable an user-friendly sEMG system, we have designed a portable circuit, as illustrated in Fig. 2A. The dimensions of the acquisition circuit are 23 mm in width and 56 mm in length, with a weight of 7.5 g. The sEMG system was developed not only for portable testing in hospitals, but also for some wearable applications. Importantly, the lightweight of this circuit also meets the requirement of wearing comforts.

Obtaining high-quality EMG signals is not a straightforward task, primarily due to the fact that EMG signals constitute a type of minute signal characterized by high source impedance. Consequently, we have iteratively refined and optimized the data acquisition system multiple times to address this challenge. The hardware block diagram of the circuit is depicted in Fig. 2B. This diagram displays two primary interfaces that connected with the external environment: an eight-channel EMG input interface and a Bluetooth wireless data transmission interface.

For EMG input and acquisition, an integrated ADC chip (ADS1198) was used. Although the conventional approach involves employing discrete components to filter and amplify the EMG signals, subsequently utilizing the ADC of MCU for signal collection, two primary challenges still exist:

1) Increased PCB board area: The use of discrete devices results in an expanded PCB board area, which hampers the pursuit of miniaturization and integration.

2) ADC accuracy limitation: The Successive Approximation Register (SAR) ADC featured in the MCU entails limited accuracy, rendering it suboptimal for our needs. By utilizing ADS1198 physiological electrical signal acquisition chip, circuit miniaturization, acquisition accuracy, and isolation of superior analog from digital signal during the PCB layout process can be achieved. This is a critical step in achieving a portable and lightweight sEMG system.

For data transmission, the transceiver functionality can be obtained by using a chip (STM32WB55CGU6) equipped with Bluetooth function. By leveraging this MCU, we obviate the need for a standalone Bluetooth chip, leading to a substantial reduction in the acquisition circuit's dimensions. Moreover, the inclusion of built-in Bluetooth module of the MCU fosters enhance efficiency in data exchange between the central processing unit and the Bluetooth stack. This synergy translates to a more judicious utilization of Bluetooth communication bandwidth, thereby enhancing overall performance.
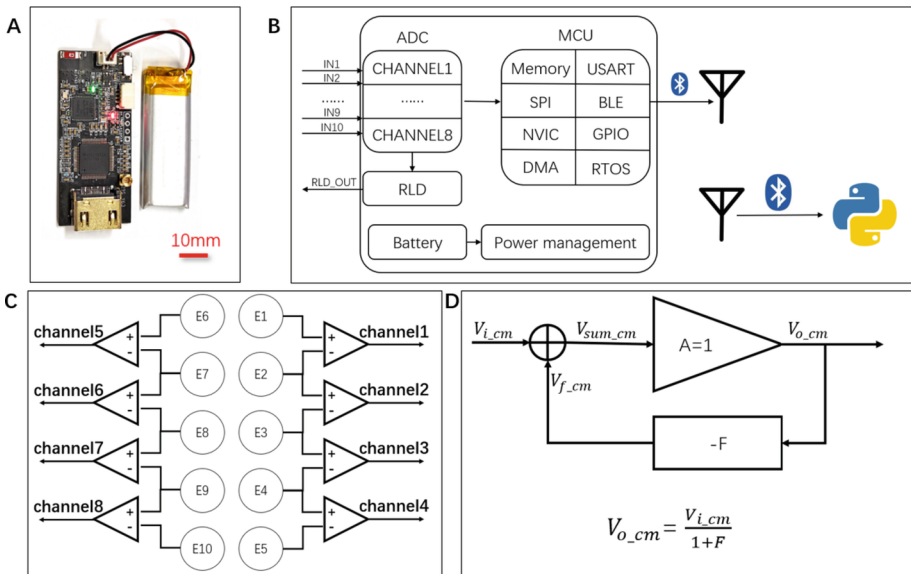
Fig. 2 Illustrates of the electromyographic signal acquisition system. (A) Physical diagram of the sEMG signal acquisition circuitry. (B) Schematic representation of the sEMG signal acquisition system, including the functions of signal collection, data packaging, and wireless transmission via Bluetooth to the user-end receiver. (C) Depiction of the attachment of electromyographic electrodes, wherein the positive and negative inputs of two adjacent channels are connected, necessitating the affixation of a total of ten electrodes for the eight-channel electromyographic signal. (D) Signal diagram of the right-foot driving module, employed for common-mode interference suppression

2.2 Electrode Attachment

The proposed electromyographic signal detection equipment facilitates the concurrent collection of 8 channels of electromyographic signals. During the detection process, electrodes are affixed to two columns along the muscle fibers, as illustrated in Fig. 2C. The EMG signal is acquired using a differential method, necessitating the use of two electrodes per channel. The positive input and negative input of adjacent channels are linked. This configuration significantly reduces the electrode count, thereby fostering a more concentrated channel arrangement. Each column accommodates a total of four channels, leading to deploy five electrodes per column, with the two adjacent electrodes jointly forming a channel.

Given the substantial impedance of human skin, the acquisition of EMG signals is susceptible to be interfered by common-mode voltage. To counteract this, we have incorporated a reference electrode to achieve voltage balance. This reference electrode is positioned on an area of human skin devoid of muscle tissue. During the testing phase, we observed that merely grounding the human body in synchronization with the acquisition device does not yield perfect suppression of common-mode interference. In response, we drew inspiration from the commonly employed right foot drive circuit (RLD) in electrocardiogram (ECG) acquisition, as illustrated in Fig. 2D. This tecnique leverages the principle of negative feedback, channeling the common-mode aspect of the collected signal back into the right foot drive module. This approach ensures that the reference potential along the entire collection pathway remains at zero, thereby significantly enhancing the suppression of common-mode voltage interference.

An additional interference that considerably impacts EMG signals is the 50 Hz / 60 Hz power frequency disturbance, arising from electromagnetic interference originating in the power mains and infiltrating the acquisition circuit as noise. The approach employed to address this issue involves the utilization of interfaces and transmission lines characterized by high degrees of shielding effectiveness. The standard ECG lead equipped with ten collection electrodes is employed. This choice hinges on the lead's robust shielding layer, which serves to curtail the ingress of interference. In terms of interfaces, our preference is the HDMI interface lead. In contrast to the traditional DB19 interface, the HDMI interface has a more compact form fact. For the RLD drive electrode, we have implemented a shielded lead wire for connection. The MMCX interface is skillfully integrated, welding it to establish a link between the lead and the acquisition circuit. MMCX interface is commonly employed for transmitting audio signals in earphones, showcasing compact physical dimensions with exemplary signal shielding capabilities.

3   Data Collection

Upon finalizing the design of acquisition system, we start formulating the data collection strategy. Our primary objective includes the EMG data collection from elderly individuals afflicted with sarcopenia, juxtaposed with EMG data collection from a reference group of normal elderly individuals.

Following comprehensive analysis and rigorous testing, the bicep muscle emerged as the chosen test muscle. This selection was grounded in several pivotal factors: 1)

The bicep muscle's attachment area was devoid of other muscles, ensuring that the collection process remained unaffected by interference from neighboring muscles. 2) The bicep muscle's force action was relatively straightforward and easily quantifiable, rendering it amenable to testing. While leg muscles are often preferred for sarcopenia [14, 15], we recognized that leg EMG signals present a testing challenge, unlike the biceps. Consequently, we made a deliberate decision to focus on the bicep muscle to facilitate targeted data collection.

During the experimental phase, we incorporated two distinct actions as our testing protocols: the Muscle Maximal Voluntary Contraction (MVC) and a Fixed Tension Test using a weight of 2 kg. As depicted in Fig. 3A, it was essential for participants to maintain vertical alignment of their forearms and upper arms throughout the testing. The MVC test served the purpose of standardizing the amplitude of EMG. The 2 kg fixed tension test required participants to sustain the posture illustrated in Fig. 3B for a duration of 2 m. Throughout this period, continuous EMG signal data were recorded. Thus, each participant yielded a set of both MVC signals and fixed tension test signals.
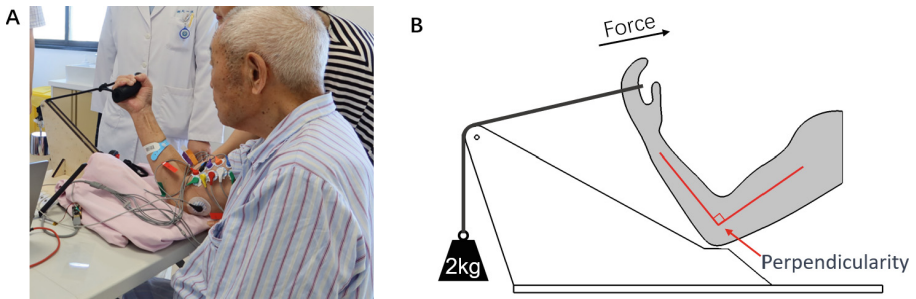
Fig. 3 Electromyographic signal acquisition schematic. (A) Photograph taken during the electromyographic signal collection at the hospital, illustrating electrodes attached to the biceps brachii, wherein the participant's muscle contraction is employed to lift a weight. (B) Illustrative diagram of the testing setup, requiring the forearm to be perpendicular to the upper arm

In the preliminary testing phase, we also explored incorporating repetitive dumbbell lifts as a testing action. However, due to challenges related to the cognitive capabilities of elderly participants, many struggled to complete the exercise test according to the stipulated standards. Consequently, we opted not to include this action in our final testing regime.

The corresponding EMG signals acquisition from participants have been approved by ethical committees of the 1st affiliated hospital of Zhejiang University. The related electrodes placement on human participants and the collection of EMG signals were conducted by professional medical staffs. We finally left 15 participants, eight of whom were diagnosed with sarcopenia, while others represented healthy individuals.

4   Data Analysis

4.1   Preconditioning

The original EMG signals inherently exhibit baseline drift and are susceptible to noise interference. The extraction of accurate, stable, and dependable information from the original EMG signal necessitates the elimination of these sources of interference, thereby facilitating subsequent analysis. The initial step is to eliminate baseline drift from the electromyographic signals. Both the moving average and wavelet transform techniques are capable of extracting baseline components from the EMG signals. By subtracting the baseline-extracted EMG signal from the original, an EMG signal devoid of baseline drift can be obtained. However, we opted for a simpler strategy: high-pass Butterworth filter.

Given that EMG signals primarily occupy the frequency range of 6 to 400 Hz, with the majority of energy concentrated between 20 and 150 Hz [16], the utilization of a 6–400 Hz bandpass Butterworth filter effectively removes extraneous components. Recognizing baseline drift as low-frequency noise, its elimination is seamlessly accomplished through bandpass filtering. Subsequent fast Fourier transform analysis of the bandpass-filtered EMG unveils conspicuous spikes corresponding to 50 Hz and its harmonics. This phenomenon led to deduce that despite the incorporation of shielding during the electromyographic signal acquisition process, a fraction of power-line interference has nonetheless infiltrated the signal. To counter this, we implemented notch filtering at frequencies such as 50 Hz and 150 Hz. With these steps, we arrived at a relatively untainted EMG signal, poised for subsequent analysis.

4.2   Feature Extraction

The gamut of features extractable from EMG encompasses time domain features, frequency domain features, and nonlinear features. When delving into time domain features, the utilization of MVC test outcomes is indispensable to normalize EMG amplitude obtained during sustained tension tests. This corrective action is mandated by the variations in individuals' skin thickness and adipose tissue content, which significantly influence EMG amplitude. The exploration of frequency domain indices requires the Fourier transform of the EMG signal. Nonlinear features have emerged as electromyographic signal analysis features in recent years. They have demonstrated significant efficacy in the domain of muscle fatigue assessment [17]. Consequently, we have also harnessed the potential of fractal dimension features extracted from the EMG for analysis endeavors. Specifically, the box dimension algorithm is employed to calculate fractal dimension values. In sum, we extracted fractal dimension (FD), median frequency (MF), root mean square (RMS), variance (VAR), kurtosis (KUR), and peak-factor (PF) from the EMG signal. In the hospital-based assessments, we additionally employed BIA to evaluate participants' ASM. Comprehensive results are displayed in Table 1.

Table 1. The clinical indices and electromyographic characteristics of each participant

| ID	Age	Type	ASM	FD	MF	RMS	VAR	KUR	PF
1	85	S	3.93	1.59	103.85	0.119	0.0152	4.16	4.19
2	83	H	8.07	1.58	84.90	0.075	0.0057	3.41	3.75
3	88	H	6.91	1.58	81.04	0.146	0.0220	3.38	3.74
4	89	S	5.6	1.59	90.70	0.080	0.0066	3.38	3.75
5	86	S	3.41	1.58	115.47	0.066	0.0053	5.07	4.56
6	81	H	5.81	1.58	85.85	0.084	0.0078	3.46	3.84
7	91	S	3.39	1.60	114.00	0.091	0.0092	3.99	4.15
8	94	S	5.51	1.59	115.18	0.244	0.0630	4.64	4.43
9	92	H	6.77	1.59	95.90	0.085	0.0081	3.47	3.83
10	72	S	4.94	1.60	104.99	0.100	0.0118	3.59	3.90
11	83	S	5.34	1.59	91.07	0.090	0.0082	3.32	3.71
12	93	S	4.5	1.59	100.28	0.163	0.0290	3.64	3.94
13	94	H	5.89	1.60	98.72	0.174	0.0315	3.47	3.84
14	90	H	7.81	1.57	83.05	0.121	0.0151	3.55	3.88
15	87	H	5.72	1.59	85.70	0.053	0.0034	3.30	3.61

[*] S = Sarcopenia; H = Healthy People

4.3   Results

While deep learning and machine learning have gained wide attentions in EMG signal analysis, particularly in the realm of motion recognition [18, 19], their reception in the medical domain remains relatively reserved. On the other hand, traditional mathematical and statistical methodologies are often preferred due to their higher degree of comprehensibility. Such approaches allow medical professionals to gain a clearer understanding of how a model reaches conclusions, enhancing applicability in clinical practice. Thus, when analyzing the relationship between electromyography and sarcopenia, we adopt mathematical techniques for feature extraction and employed statistical methods to investigate correlations between electromyography features and established clinical features.

The analysis encompassed the correlation between the six features derived from the EMG signal and ASM from BIA. Eventually, a good linear correlation between the median frequency and body composition is achieved (Fig. 4). This correlation shows a coefficient of 0.774 with a significant p-value of 0.001.

The calculation process of MF is relatively straightforward. It involves transforming a time-domain signal within a time window into a frequency-domain signal using Fourier transformation. The frequency at which the power on both sides of the spectrum is equal is defined as the median frequency. Fortunately, the efficiency of calculation is significantly improved by the FFT (Fast Fourier Transform). In the future, there is potential for the integration of this algorithm within the data acquisition system, enabling offline analysis
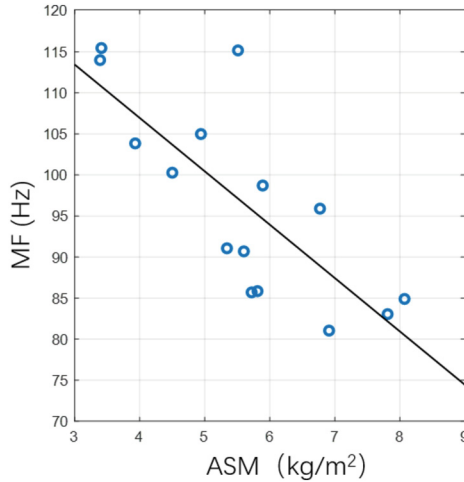
Fig. 4 Relationship between electromyographic median frequency and appendicular skeletal muscle mass (ASM), correlation = 0.774, p < 0.001, N = 15

of sarcopenia. The utilization of median frequency analysis of ASM has the potential to substantially streamline the detection process and reduce testing costs.

5   Conclusion

To address the challenges encountered in sarcopenia diagnosis, particularly the expensive and non-portable nature of ASM testing equipment, an electromyographic signal acquisition system is developed for sarcopenia assessment. This innovative system enables eight-channel sampling at a high 2 kHz rate, with real-time transmission to a personal computer via Bluetooth. Leveraging this technology, EMG signals are successfully collected from 15 elderly women with the extraction of six distinct characteristic values. Notably, the median frequency exhibits a robust correlation with body composition. The electromyography feature obtained through this testing methodology holds the potential as an alternative benchmark for body composition assessment towards future clinical standards.

Beyond its diagnostic applications, this collection system has the potential to transition into a community-level device for large-scale sarcopenia screening. Its deployment can significantly contribute to early sarcopenia diagnosis, extending the benefits of timely intervention to a broader demographic.

References

1. Rosenberg, I.H.: Sarcopenia: origins and clinical relevance. J. Nutr. **127**(5), 990S–991S (1997)
2. Boirie, Y.: Physiopathological mechanism of sarcopenia. JNHA - J. Nutr. Health Aging **13**(8), 717–723 (2009)

3. Landi, F., et al.: Sarcopenia as a risk factor for falls in elderly individuals: results from the ilSIRENTE study. Clin. Nutr. **31**(5), 652–658 (2012)
4. Tarantino, U., et al.: Osteoporosis and sarcopenia: the connections. Aging Clin. Exp. Res. **25**, 93–95 (2013)
5. Landi, F., et al.: Sarcopenia and mortality risk in frail older persons aged 80 years and older: results from ilSIRENTE study. Age Ageing **42**(2), 203–209 (2013)
6. Chen, L.-K., et al.: Asian working group for sarcopenia: 2019 consensus update on sarcopenia diagnosis and treatment. J. Am. Med. Directors Assoc. **21**(3), 300–307.e2 (2020)
7. Cruz-Jentoft, A.J., et al.: Sarcopenia: revised European consensus on definition and diagnosis. Age Ageing **48**(1), 16–31 (2019)
8. Sergi, G., De Rui, M., Stubbs, B., Veronese, N., Manzato, E.: Measurement of lean body mass using bioelectrical impedance analysis: a consideration of the pros and cons. Aging Clin. Exp. Res. **29**, 591–597 (2017)
9. Hioka, A., Akazawa, N., Okawa, N., Nagahiro, S.: Extracellular water-to-total body water ratio is an essential confounding factor in bioelectrical impedance analysis for sarcopenia diagnosis in women. Eur. Geriatr. Med. **13**(4), 789–794 (2022)
10. Norali, A.N., Som, M., Kangar-Arau, J.: Surface electromyography signal processing and application: a review. In: Proceedings of the International Conference on Man-Machine Systems (ICoMMS), no. 11–13 (2009)
11. Garcia, M.C., Vieira, T.M.M.: Surface electromyography: why, when and how to use it. Revista andaluza de medicina del deporte **4**(1), 17–28 (2011)
12. Reaz, M.B.I., Hussain, M.S., Mohd-Yasin, F.: Techniques of EMG signal analysis: detection, processing, classification and applications. Biological Proced. Online **8**, 11–35 (2006)
13. Balbinot, G., Li, G., Wiest, M.J., Pakosh, M., Furlan, J.C., Kalsi-Ryan, S., Zariffa, J.: Properties of the surface electromyogram following traumatic spinal cord injury: a scoping review. J. NeuroEngineering Rehabil. **18**(1), 105 (2021)
14. Fialkoff, B., et al.: Hand grip force estimation via EMG imaging. Biomed. Signal Process. Control **74**, 103550 (2022)
15. Chen, I., et al.: Sarcopenia recognition system combined with electromyography and gait obtained by the multiple sensor module and deep learning algorithm. Sens. Mater. **34**(6), 2403 (2022)
16. Webster, J.: Medical Instrumentation: Application and Design, Wiley (2010)
17. Rampichini, S., et al.: Complexity analysis of surface electromyography for assessing the myoelectric manifestation of muscle fatigue: a review. Entropy **22**(5), 529 (2020)
18. Moin, A., et al.: A wearable biosensing system with in-sensor adaptive machine learning for hand gesture recognition. Nat. Electron. **4**(1), 54–63 (2021)
19. Tang, W., et al.: Delamination-resistant imperceptible bioelectrode for robust electrophysiological signals monitoring. ACS Mater. Lett. **3**(9), 1385–1393 (2021)